IR Spectroscopic Features of Gaseous $C_7H_7O^+$ Ions: Benzylium versus Tropylium Ion Structures

Barbara Chiavarino,* Maria Elisa Crestoni, and Simonetta Fornarini

Dipartimento di Studi di Chimica e Tecnologia delle Sostanze Biologicamente Attive, Università di Roma "La Sapienza", P.le A. Moro 5, I-00185 Roma, Italy

Otto Dopfer

Institut für Atomare Physik und Fachdidaktik, Technische Universität Berlin, Hardenbergstrasse 36, D-10623, Berlin, Germany

Joel Lemaire and Philippe Maître

Laboratoire de Chimie Physique, UMR8000 CNRS and Université Paris Sud 11, Faculté des Sciences d'Orsay, Bâtiment 350, 91405 Orsay Cedex, France

Received: May 9, 2006; In Final Form: June 5, 2006

Gaseous $[C_7H_7O]^+$ ions have been formed by protonation of benzaldehyde or tropone (2,4,6-cycloheptatrienone) in the cell of an FT-ICR mass spectrometer using $C_2H_5^+$ as a Brønsted acid. The so-formed species have been assayed by infrared multiphoton dissociation (IRMPD) using the free electron laser (FEL) at the CLIO (Centre Laser Infrarouge Orsay) facility. The IRMPD features are quite distinct for ions from the two different precursors, pointing to two different isomers. A number of potential structures for $[C_7H_7O]^+$ ions have been optimized at the B3LYP/6-31+G(d,p) level of theory, and their relative energies and IR spectra are reported. On this basis, the IRMPD spectra of $[C_7H_7O]^+$ ions are found to display features characteristic of O-protonated species, with no evidence of any further skeletal rearrangements. The so-formed ions are thus hydroxy-substituted benzylium and tropylium ions, respectively, representative members of the benzylium/tropylium ion family. The IRMPD assay using the FEL laser light has allowed their unambiguous discrimination where other mass spectrometric techniques have yielded a less conclusive answer.

Introduction

Considerable interest is attached to the gaseous ions that are obtained by protonation of simple aromatic molecules, such as benzene or its monosubstituted derivatives (E-C_6H_5). Their intrinsic features, such as structure, spectroscopic properties, reactivity, and energetics, obtained in the gas phase may be evaluated directly against the results of theoretical calculations on isolated species and, ultimately, may lead to an understanding of their role as reaction intermediates in more complex environments. E-C_6H_5 is potentially a polyfunctional base. Protonation at a ring carbon yields E-substituted arenium ions, established intermediates in electrophilic aromatic substitution reactions.[1] Alternatively, the E-group itself may be protonated. This reaction becomes a likely possibility when E is an electron-withdrawing substituent, such as the formyl group, CHO, endowed with substantial basicity, exerting at the same time a deactivating effect on the aromatic ring. In this study the $[C_7H_7O]^+$ ion obtained in the gas phase by protonation of benzaldehyde is examined by an IR spectroscopic technique. Characterizing the structures of gaseous protonated aromatic compounds is not a trivial problem.[2] Several different approaches have been used to identify a variety of possible $[C_7H_7O]^+$ isomers, differing either for the position of a hydrogen atom or for the heavy atom skeleton, including photodissociation (PD), ion−molecule reactions, collisionally activated dissociation, and metastable ion studies.[3] Also sequential H/D exchange reactions by gaseous protonated aromatics have been exploited to obtain information on the number of ring carbon atoms involved in proton attachment.[4] Using this tool, the reaction of arenium ions with H/D exchange reagents investigated at atmospheric pressure by a radiolytic technique has disclosed the favored protonation sites of exemplary aromatics and evidence was obtained that E-C_6H_5 undergoes predominant protonation on the substituent when E is an electron-withdrawing group such as CF_3CO.[5] However, a spectroscopic method appears highly desirable for assessing the structural and bonding features of gaseous ions from aromatic molecules. In fact, using spectroscopic techniques one may minimize the perturbation that is necessarily involved when a species is assayed by a reactivity probe. At the same time, spectroscopic investigations in the IR region of the electromagnetic spectrum can be highly informative about the structure of the sampled species. Detailed information on the IR spectroscopic features of relatively complex species such as the ions derived from aromatic molecules has become accessible by the recent developments of tunable IR laser technology combined with various mass spectrometric methodologies.[6] The ensuing spectroscopic techniques are based on the detection of a dissociation process activated by photon absorption in resonance with an active vibrational mode. One needs to note, however, that the absorption of a single photon in the IR energy range is typically inadequate in inducing the dissociation of the bare

* Corresponding author. E-mail: barbara.chiavarino@uniroma1.it. Fax: (+39) 06-4991-3602. Phone: (+39) 06-4991-3634.

10.1021/jp0628380 CCC: $33.50
Published on Web 07/13/2006

cations of ionized or protonated aromatic molecules, necessarily implying the cleavage of strong covalent bonds. To circumvent this problem, a "messenger" technique has been devised by Lee and co-workers,[7] based on the formation of a van der Waals cluster of the ion of interest with an inert, loosely bound species such as a rare gas atom. By this approach IR absorption features of several representative cationic aromatic and heteroaromatic molecules[8] and arenium ions[9] have been described. Alternatively, IR spectroscopic information on the naked ions from aromatic molecules has been obtained using high-intensity laser fields to induce resonance enhanced multiple photon absorption and achieve photodissociation (IRMPD) along routes involving rupture of strong covalent bonds. The intense and narrow-band IR radiation of a free electron laser (FEL) has been exploited to obtain IRMPD spectra of ionized polycyclic aromatic hydrocarbon molecules at the FELIX (Free Electron Laser for Infrared Experiments) center[6f,10] and of protonated benzene and monosubstituted benzenes at the CLIO (Centre Laser Infrarouge d'Orsay) facility.[11] This methodology has proven to be well suited for studying the vibrational spectrum of cationic arylcarbonyl compounds such as the benzoic acid and *para*-aminobenzoic acid radical cations and their dehydroxylated fragment ions.[12] In this study $[C_7H_7O]^+$ ions were formed by protonation of benzaldehyde in a compact FT-ICR analyzer,[13] where they were isolated, stored, and exposed to IRMPD using the CLIO IR laser beam.[14] To substantiate the interpretation of the so-obtained IRMPD spectrum, $[C_7H_7O]^+$ ions were obtained also by protonation of tropone (2,4,6-cycloheptatrienone, a constitutional isomer of benzaldehyde) and submitted to the same spectroscopic assay. The gas phase protonation of these neutrals was expected to provide a source of hydroxy-substituted benzyl and tropylium ions, and an unambiguous structural assignment on the basis of their IR spectral features was sought. The valuable tool of IRMPD spectroscopy for the characterization of gaseous reactive intermediates finds a parallel in condensed phases, where the identification of charged species from aromatic compounds, such as the reactive intermediates in the electrophilic substitution reaction, has largely relied on spectroscopic methods, especially NMR and IR techniques.[1a] In a recent achievement, X-ray crystallography has been applied as well,[15] a step further toward the goal of the thorough understanding of the bonding and reactivity features of reactive intermediates in different environments. It needs to be stressed, though, that isolated species assayed in a dilute gaseous environment are least affected by perturbations due to counterion, solvent, or crystalline network. This work aims to uncover some of their intrinsic features.

Experimental Section

The IRMPD experiments were performed with an experimental platform[14] combining a movable ICR analyzer (MICRA)[13] with the radiation output of the CLIO FEL.[16] At the core of MICRA, an open cubic cell (2 cm side) placed within a 1.24 T permanent magnet allows the entrance of the IR FEL beam through a ZnSe optical window. The irradiation time is set by a fast electromechanical shutter which is synchronized with the FEL. The IR FEL at CLIO is based on a 10−50 MeV electron accelerator and provides radiation continuously tunable over the 3−90 μm range with a relative bandwidth (fwhm) of 0.3−0.5%. In this work we investigated the range between 670 and 1850 cm^{-1} using the FEL beam operated with an electron energy of 40 or 45 MeV. The CLIO FEL IR radiation is structured in series of macropulses, 8 μs long, delivered at a repetition rate of 25 Hz. Each macropulse conveys a train of 500 micropulses, each a few ps long, 16 ns from each other. With a typical mean IR power of 500 mW, micropulse and macropulse energies are 40 μJ and 20 mJ, respectively. The same sequence of events was adopted to form $[C_7H_7O]^+$ ions by protonation of either benzaldehyde or tropone. Protonating species, CH_5^+ and $C_2H_5^+$, were obtained by ionization of methane, pulsed into the cell at 3.3×10^{-7} mbar, and ensuing ion−molecule reactions. $C_2H_5^+$ ions were isolated by resonant radio frequency ejection techniques. Benzaldehyde or tropone was then pulsed in at 1.0×10^{-6} mbar, and a 0.5 s delay was allowed for the proton transfer to occur. The ions of interest were mass selected, allowed to relax to thermal equilibrium with the environment during a 2 s delay time, and finally irradiated for 1 s. A mass spectrum was derived at each wavelength from an ion signal averaged over four sequences, and the radiation wavelength was scanned in steps of 6 cm^{-1}. When in resonance with an active vibrational mode of the sampled species, the absorption of multiple photons may heat the ion up to the critical energy for a dissociation process and both parent and photofragment ions will appear in the mass spectrum. An IRMPD spectrum is obtained when the IRMPD yield, $R = -\log [I_{parent}/(I_{parent} + \Sigma I_{fragment})]$, is plotted as a function of the photon wavenumber in the selected range. It should be noted that considering the behavior of R as a function of the laser intensity, no posttreatment was applied in order to correct for the IR−FEL intensity variations.

Molecular structures and relative energies for several isomeric $[C_7H_7O]^+$ ions and related species were calculated using hybrid density functional theory (B3LYP) and the 6-311+G(d,p) basis set in the frame of the Spartan '04 (revision 1,0,0; Wavefunction Inc.) software. Vibrational analysis was performed to ensure that the computed structures of the various isomers lie in energy minima and to obtain their IR spectra. The interpretation of the IRMPD spectra of $[C_7H_7O]^+$ ions is based on the comparison with calculated IR absorption spectra obtained at the same level of theory. Hybrid DFT methods such as B3LYP are recognized to perform well in describing IR spectra in terms both of wavelength and of relative intensity of absorption bands. However, scaling factors are normally used to account for anharmonicity. Uniform scaling factor values of 0.96−1.0 have been recommended for vibrational frequencies determined at the B3LYP level using a saturated basis set. It should be noted however that if the highly anharmonic X−H stretching modes (X = C, N, O), typically higher than 1800 cm^{-1}, are omitted, the value of a specifically optimized scaling factor for vibrational frequencies lower than 1800 cm^{-1} calculated using a hybrid DFT level ranges between 0.98 and 1.0.[17c] In this work, a value of 0.98 was used to scale the calculated vibrational frequencies in the 670−1850 cm^{-1} wavenumber range.

Results and Discussion

Protonated Benzaldehyde. $[C_7H_7O]^+$ ions have been obtained by the gas-phase protonation of benzaldehyde in the MICRA cell effected by $C_2H_5^+$ ions (eq 1), according to a process exothermic by 153.5 kJ/mol:[18]

$$C_2H_5^+ + C_6H_5CHO \rightarrow [C_7H_7O]^+ + C_2H_4 \qquad (1)$$

Although the thermodynamically favored protonation site is known to be the oxygen atom,[19] the energy released in the reaction may give access to carbon-protonated isomers as well. Indeed, the choice of the protonating agent was suggested by the possibility to sample in principle both O and C protonation sites. Chart 1 shows the ions corresponding to protonated

CHART 1

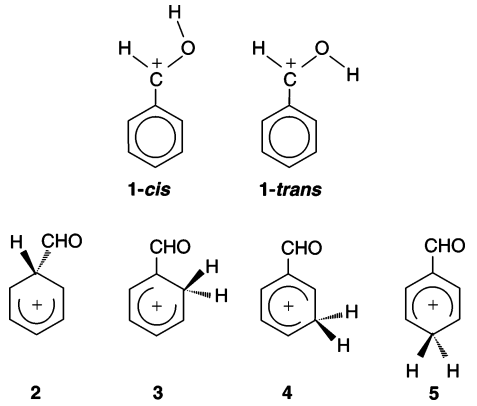

TABLE 1: Computed Energies of Isomeric $[C_7H_7O]^+$ Ions and Fragmentation Products

species	rel enthalpy[a]
1-*cis*	0 (0)
1-*trans*	10.5
$TS_{cis/trans}$	66.1
2	130.3 (132.2)
3	112.2 (111.1)
4	116.2 (116.8)
5	118.9 (117.5)
6	14.9
7	168.1
8	41.3
9	76.5
10	24.0
$PhCHO + H^+$	841.2
$c\text{-}C_7H_6O^b + H^+$	935.0
$C_6H_7^{+c} + CO$	91.9
$C_6H_5^{+d} + H_2CO$	350.9

[a] In kJ/mol at 0 K. A scaling factor of 0.98 was applied to zero point energy (ZPE) values. All calculations were performed at the B3LYP/6-311+G(d,p) level. Differences in zero point and 298 K energies are identical within ±2 kJ/mol; thus, the relative energies also apply to 298 K. Recent literature values obtained at the 1MP2/6-31G(d) level of theory are given in parentheses.[19b] [b] Tropone (2,4,6-cycloheptatrienone). [c] Benzenium ion. [d] Phenyl cation.

benzaldehyde (**1**−**5**). Their absolute and relative energies are summarized in Table 1, together with data for other $[C_7H_7O]^+$ isomers, for C_7H_6O neutrals, and for possible dissociation products. Protonation on the carbonyl oxygen yields two isomers (**1**-*cis* and **1**-*trans*) in which the proton is either cis or trans to the hydrogen on the adjacent carbon. The cis form is found to be dominant when benzaldehyde is protonated in strong superacids,[20] where O-protonation is the only process observed. As shown in Table 1, **1**-*cis* is more stable than **1**-*trans* by 10.5 kJ/mol, in agreement with a 9.2 kJ/mol enthalpy difference obtained at the MP2/6-31G*//MP2/6-31G* level of calculations.[20] Incidentally, the fact that oxygen protonation is favored also in the gas phase is confirmed by the agreement between the experimental value for the proton affinity of benzaldehyde (834.0 kJ/mol)[18] and the value of 841.2 kJ/mol obtained by the present B3LYP/6-311+G(d,p) calculations assuming **1**-*cis* as the protonated species. The two species are separated by a substantial energy barrier associated to the rotation around the C−O bond. The transition state ($TS_{cis/trans}$) for the **1**-*cis* → **1**-*trans* process is 66 kJ/mol higher in energy relative to **1**-*cis* (Table 1). The C−O bond displays significant double bond character due to electron release from oxygen to the neighboring carbon, and **1**-*cis* and **1**-*trans* are in fact best described as carboxonium ions rather than as carbenium ions as formally depicted in Chart 1.[20,21]

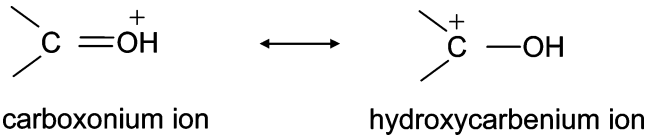

The ring protonated isomers are all much higher in energy although the formation of **2**−**5** may be accessed using a strong acid such as $C_2H_5^+$. It is worth mentioning that the properties reported in Table 1 pertain to the minimum energy structure for each isomer. For example, the lowest-energy conformation of *ortho* protonated benzaldehyde **3** has the C═O bond anti with respect to the tetrahedral ring carbon; however, the energy difference with the conformation bearing a formyl group rotated by 180° (not reported in Table 1) is only 8 kJ/mol.

When the so-formed $[C_7H_7O]^+$ ions are probed by IRMPD, efficient photofragmentation is observed depending on the photon wavenumber. When the 670−1700 cm^{-1} region is scanned, two fragmentation channels are observed at a measured average power of 900 mW, leading to $C_6H_7^+$ and $C_6H_5^+$ ions by loss of CO and $[H_2CO]$ neutrals, respectively (Figure 1). The loss of CO from **1**-*cis* is estimated to be endothermic by 91 kJ/mol, assuming a benzenium ion structure for the $C_6H_7^+$ fragment, using the computational results reported in Table 1 (or 120 kJ/mol using available experimental data).[18] To reach the dissociation energy threshold, an ion in the ground vibrational state should increase its internal energy content by absorbing at least six photons at 1300 cm^{-1}, the wavenumber range in proximity of one of the major observed IRMPD features. The loss of formaldehyde, possibly accounting for the $[H_2CO]$ fragment, is highly energy demanding, being endothermic by 350 kJ/mol, if $C_6H_5^+$ is assigned the structure of a phenylium ion (Table 1) (or 378 kJ/mol using available experimental data).[18] This fragmentation behavior is not unprecedented. The high-energy collision-induced dissociation of the $[C_7H_7O]^+$ ion generated from the protonation of benzaldehyde was found to proceed by loss of CO and $[H_2CO]$ in comparable amounts.[3a] The same fragment ions are formed in the unimolecular dissociation reactions of $[C_7H_7O]^+$ ions from various precursors, although the results of metastable ion studies were not considered conclusive as to the identification of the structure and possible rearrangement reactions of protonated benzaldehyde.[3b] Interestingly, however, the unimolecular dissociation of metastable $[C_7H_7O]^+$ ions from benzyl alcohol proceeds by exclusive loss of CO. The mechanism for the loss of CO from O-protonated benzaldehyde (**1**) was suggested to be stepwise, involving a hydrogen shift to form the *ipso*-protonated isomer **2**, followed by C−C bond cleavage yielding an ion−neutral complex of the formyl cation with benzene.[22] Proton transfer to benzene should finally give the end products, $C_6H_7^+$ and CO. It may be further noted that the profiles of ion abundances reported in Figure 1, besides showing an extensive depletion of the sampled $[C_7H_7O]^+$ ions, appear to indicate that the relative yield of $C_6H_7^+$ and $C_6H_5^+$ fragment ions depends on the photon wavenumber. Mode-specific photofragmentation behavior has been reported and suggested to reflect the complex sequence of multiphoton absorption and fragmentation dynamics.[12b,23,24] In the present case, the possibility should be considered that the loss of $[H_2CO]$ may result from a stepwise process involving consecutive CO and H_2 losses. When the same wavenumber range is scanned with a laser power reduced to an average value of 420 mW (Figure 2), the $[H_2CO]$ loss channel is practically suppressed. This result may be considered as circumstantial evidence that the primary $C_6H_7^+$ photofragment may undergo a subsequent photodissociation process losing H_2.

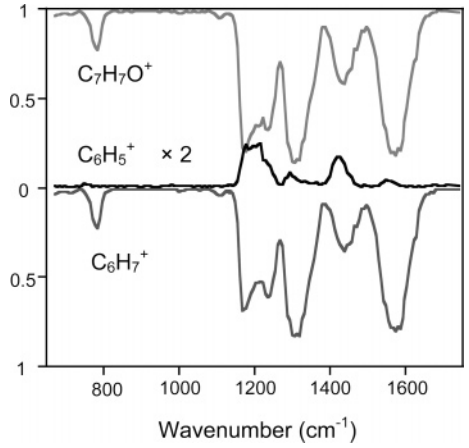

Figure 1. Ion abundances (in arbitrary units) for $[C_7H_7O]^+$ (protonated benzaldehyde) and for the fragmentation products ($C_6H_7^+$ and $C_6H_5^+$, the abundance of $C_6H_5^+$ expanded by a factor of 2) plotted as a function of IR wavenumber (laser power = 900 mW).

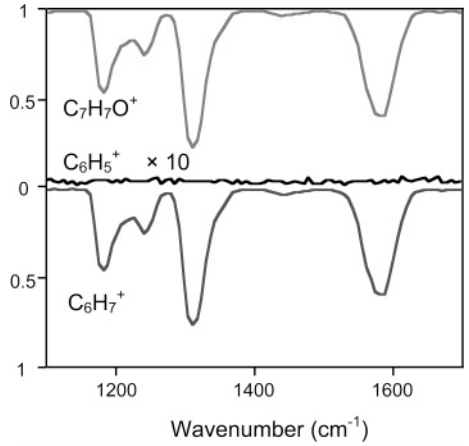

Figure 2. Ion abundances (in arbitrary units) for $[C_7H_7O]^+$ (protonated benzaldehyde) and for the fragmentation products ($C_6H_7^+$ and $C_6H_5^+$, the abundance of $C_6H_5^+$ expanded by a factor of 10) plotted as a function of IR wavenumber, using an attenuated laser beam (laser power = 420 mW).

In fact, this secondary photodissociation process leading to $C_6H_5^+$ becomes especially evident in correspondence with the two major IRMPD features of protonated benzene, namely in proximity of two IR active bands of $C_6H_7^+$ at 1228 and 1433 cm^{-1}.[11a] The profiles of ion abundance for the $C_6H_7^+$ and $C_6H_5^+$ fragment ions are shown in the 1100−1700 cm^{-1} range in Figure 3, also reporting the IRMPD spectrum of protonated benzene in the same wavenumber range (gray profile). The appearance of $C_6H_5^+$ as fragment ion around these specific wavenumbers then suggests a benzenium ion structure for the $C_6H_7^+$ product ion from IRMPD of protonated benzaldehyde. The formation of $C_6H_5^+$ is, on the other hand, negligible in other highly active bands of protonated benzaldehyde such as the ones observed at 1312 and 1582 cm^{-1}, rather excluding a possible origin of $C_6H_5^+$ by a competitive direct loss of H_2CO from $[C_7H_7O]^+$ ions as resulting from an enhanced rate of photon absorption.

The overall IRMPD spectrum of protonated benzaldehyde reporting the yield *R* as a function of the photon wavenumber is shown in Figure 4a. The wavenumber range from 670 to 1850 cm^{-1} was explored with an average laser power of 900 mW to reveal the highest number of significant IRMPD features, possibly including weakly active modes. The second profile in Figure 4a comprises the wavenumber range of 1000−1700 cm^{-1}, including the most pronounced bands, and was obtained

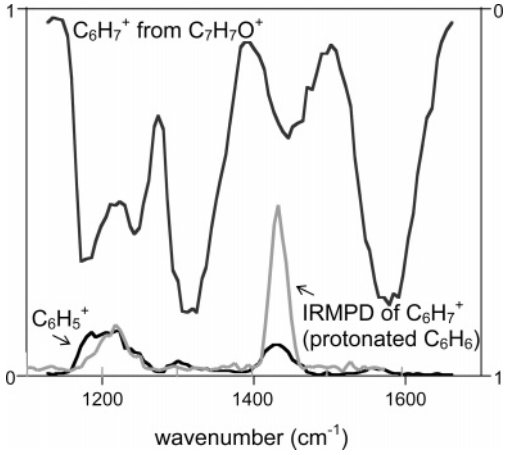

Figure 3. Ion abundances (in arbitrary units) for the formation of $C_6H_7^+$ (ordinate on the right) and $C_6H_5^+$ (ordinate on the left) by IRMPD of protonated benzaldehyde, displayed together with the IRMPD spectrum of protonated benzene.[11a]

using a reduced average laser power of 420 mW, to diminish possible saturation effects and, as noted above, to avoid secondary photofragmentation of the primary dissociation products. The other windows in Figure 4 report the calculated (scaled) IR spectra of ring-protonated isomers (**2**−**5**) as well as those of **1**-*cis* **and 1**-*trans*. In the former species (**2**−**5**) the presence of a carbonyl group is responsible for the characteristic absorption band due to the C═O stretching mode in the 1700−1800 cm^{-1} range. However, the experimental IRMPD spectrum of $[C_7H_7O]^+$ ions from protonated benzaldehyde is remarkably flat in this wavenumber range. The C═O stretching mode is known to be strongly active, as observed for example in the IRMPD spectrum of benzoic acid radical cation,[12a] and the lack of any feature in this wavenumber region, especially when using the highest fluence of the IR−FEL, is strong indication that species **2**−**5** are not present in the sampled ion population. The experimental IRMPD spectrum is in rather good qualitative agreement with the calculated IR spectrum of **1**-*cis*. The spectrum is dominated by a distinct feature at 1312 cm^{-1} which is nicely accounted for by the IR absorption band calculated at 1335 cm^{-1} corresponding to a C−OH stretching mode coupled with an in-plane C−H bending. The relatively small width of this band (fwhm ca. 30 cm^{-1}) does not support a major contribution of the **1**-*trans* isomer, which is expected to show a broad feature encompassing closely spaced active modes in the 1350−1400 cm^{-1} wavenumber region. Indeed, using the present experimental platform, IRMPD bandwidth (fwhm) typically range from 30 to 40 cm^{-1} when the ion only displays a single IR absorption band in the corresponding wavenumber region. Similarly, the observation at full laser power of an IRMPD signal at 782 cm^{-1} can clearly be attributed to a vibrational mode of **1**-*cis* calculated at 774 cm^{-1} with an intensity of ca. 60 km/mol. Other significant features, such as the broad band at 1582 cm^{-1}, or weaker features (1440 cm^{-1}) also nicely match with the IR absorption features of **1**-*cis*, but they do not provide a clear-cut diagnostic since **1**-*trans* also presents IR active modes in the same wavenumber range.

The overall IRMPD activity of $[C_7H_7O]^+$ ions from protonated benzaldehyde is noticeably high, in line with the behavior displayed by aromatic carbonyl compounds examined by the same approach.[12] The presence of **1**-*cis* as the major component of the $[C_7H_7O]^+$ ion population from protonated benzaldehyde may appear surprising if one considers the small energy difference separating **1**-*cis* and **1**-*trans* as compared with the exothermicity of the protonation event by the selected $C_2H_5^+$

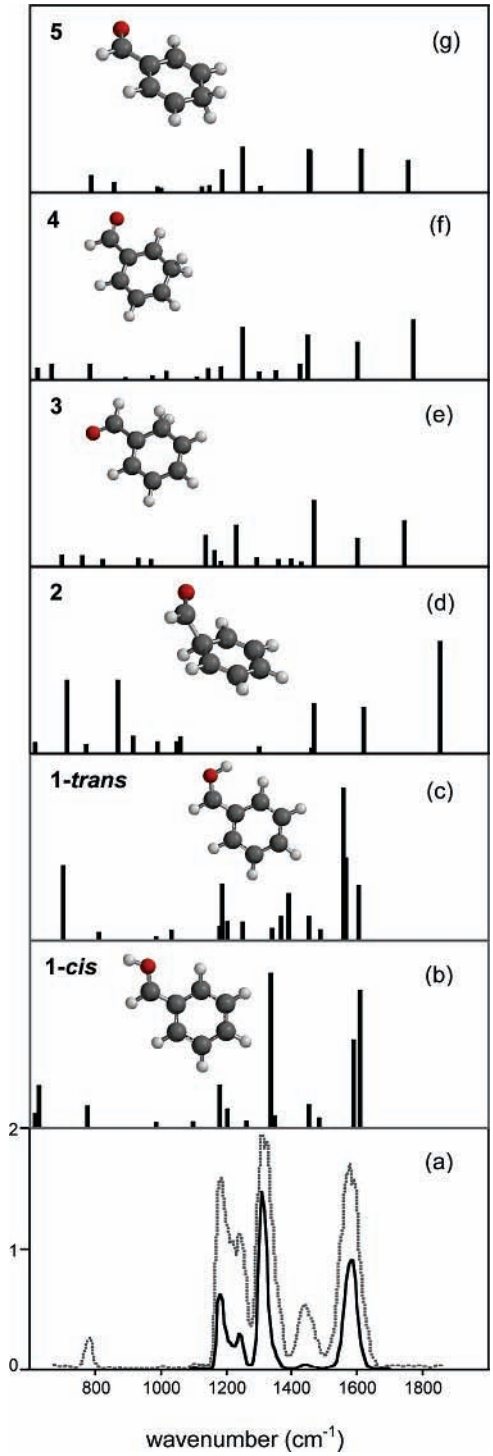

Figure 4. (a) IRMPD spectrum of $[C_7H_7O]^+$ ions from protonated benzaldehyde (*R* as a function of IR wavenumber), at full (dashed line, 900 mW) and attenuated (solid line, 420 mW) laser power. (b−g) IR stick spectra calculated for **1**-*cis*, **1**-*trans*, and **2**−**5**, respectively.

ions. It is conceivable, however, that primarily formed $[C_7H_7O]^+$ ions may react by a second proton transfer reaction with neutral benzaldehyde. Not only would the reaction become close to thermoneutral, but a steric effect may come into play, favoring the proton to be released in anti relationship with respect to the phenyl ring, thus yielding stereoselectively the **1**-*cis* isomer. Any thermal equilibration of **1**-*cis* and **1**-*trans* may then be slowed due to the significant rotational barrier separating the two isomers. At temperatures of 300−400 K, however, only a few percent fraction of **1**-*trans* should be present at equilibrium with the **1**-*cis* isomer. An indirect suggestion that the sampled ions

CHART 2

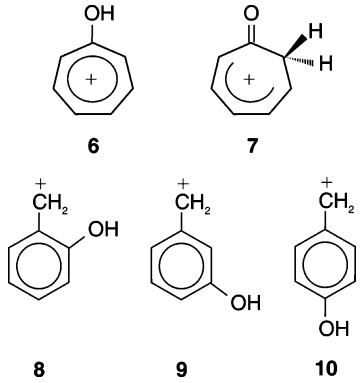

are not "hot" species comes from the relatively narrow fwhm of ca. 30 cm^{-1} that is observed for isolated bands in the IRMPD spectrum at 782 and 1312 cm^{-1}.

Protonated Tropone. On the basis of the experimental proton affinity of tropone (PA = 920.8 kJ/mol), the proton-transfer reaction from $C_2H_5^+$ ions (eq 2) is exothermic by 240.3 kJ/mol,[18] so that once again the choice of this protonating agent may allow sampling of different basic sites in the molecule and could subsequently lead to the formation of various isomers:

$$C_2H_5^+ + c\text{-}C_7H_6O \rightarrow [C_7H_7O]^+ + C_2H_4 \qquad (2)$$

According to calculations, however, the oxygen atom is by far the most basic site and protonation at this position yields the hydroxytropylium ion (**6**, Chart 2), characterized by a delocalized six π-electron system leading to considerable aromatization.[19c] Indeed, our calculated value (920.1 kJ/mol) for the proton affinity of tropone is in good agreement with the experimental value (920.8 kJ/mol). Carbon protonation, for example at C2, leads to an isomer (**7**) that is less stable by 153.2 kJ/mol (or 161 kJ/mol according to MP2/6-31G* data).[19c] Besides allowing access to carbon protonation, the energy released in the proton transfer event may conceivably allow the formation of isomers by a ring contraction process. The relative energies of the *ortho*, *meta*, and *para* isomers of the hydroxybenzyl cation (**8**−**10**) shown in Chart 2 are included in Table 1. The question of the interconversion between hydroxytropylium ion and hydroxybenzyl cations has been addressed by metastable ion techniques and thermochemical measurements providing indication that the species do not attain structural equilibration.[3] Rather, their relative population appears to be determined by their generation from a specific precursor molecule. The direct assay by IRMPD was aimed at probing the structure of the ion formed by protonation of tropone.

Similar to protonated benzaldehyde, the two dominant fragment channels observed are $C_6H_7^+$ and $C_6H_5^+$. The frequency dependence of the relative abundances of the fragmentation products along the two paths is shown in Figure 5. The branching ratio appears to be somewhat mode specific, as in the case of protonated benzaldehyde. For example, the shoulder at 1210 cm^{-1} shows a comparatively higher activity in the $C_6H_7^+$ channel than in the $C_6H_5^+$ channel with respect to other features. Furthermore, the IRMPD feature at 1450 cm^{-1} shows a distinct red shift in the $C_6H_5^+$ ion abundance profile with respect to the $C_6H_7^+$ profile. Indeed, a red shift of the $C_6H_5^+$ ion abundance profile in the shoulder at 1210 cm^{-1} may explain the apparent variation in branching ratio. On the other hand, the peak at 1167 cm^{-1} and a weak feature at 1305 cm^{-1} do not appear to show the same red shift effect. As a tentative explanation of the observed phenomena, one may conceive a

TABLE 2: Vibrational Modes of O-Protonated Benzaldehyde[a] and Experimental IRMPD Features of $[C_7H_7O]^+$ Ions from the Protonation of Benzaldehyde in the 700−1850 cm^{-1} Region

	1-*cis*[c]		**1**-*trans*[c]		exptl[d]	
vibrational mode[b]	ν	I	ν	I	ν	I_{rel}
$\beta'_{CH}\,\beta'_{OH}$	**774**	56	700	199	782	0.10
σ_{CC}			809	20		
$\beta'_{CH}\,\beta'_{OH}$			1034	26		
$\beta_{CH}\,\beta_{OH}$	**1099**	15			1100	0.01
$\beta_{CH}\,\beta_{OH}$	**1179**	114	**1180**	36	1180	0.42
$\beta_{CH}\,\beta_{OH}$			**1189**	150		
$\beta_{CH}\,\beta_{OH}$	1203	49	1200	49		
$\beta_{CH}\,\sigma_{CC}$	**1260**	17	**1247**	47	1243	0.17
$\beta_{CH}\,\sigma_{CC}$			1341	31		
$\beta_{CH}\,\sigma_{CC}$			1366	63		
$\beta_{CH}\,\sigma_{CO}$	**1336**	412	1388	124	1312	1.00
$\beta_{CH}\,\beta_{OH}\,\sigma_{CC}$			1345	30		
$\beta_{CH}\,\beta_{OH}\,\sigma_{CC}$	**1452**	61	**1450**	62	1440	0.04
$\beta_{CH}\,\sigma_{CC}$	1482	25	1489	28		
$\beta_{CH}\,\sigma_{CO}\,\sigma_{CC}$	**1589**	234	**1557**	409		
$\beta_{CH}\,\sigma_{CO}\,\sigma_{CC}$			**1566**	218		
$\beta_{CH}\,\sigma_{CC}$	**1609**	366	**1603**	146	1582	0.58

[a] B3LYP/6-311+G(d,p); frequency values are scaled by a factor of 0.98. [b] β = in plane bend; β' = out of plane bend; σ = stretch. [c] Bands with I < 15 km/mol are not included. ν in cm^{-1}; I in km/mol. The vibrational modes that may be assigned to the experimental IRMPD features are highlighted in bold. [d] ν in cm^{-1}; I_{rel} in arbitrary units.

TABLE 3: Vibrational Modes of O-Protonated Tropone[a] and Experimental IRMPD Features of $[C_7H_7O]^+$ Ions from Protonation of Tropone in the 700−1850 cm^{-1} Region

	6[c]		exptl[d]	
vibrational mode[b]	ν	I	ν	I_{rel}
β'_{CH}	767	56		
$\beta_{CH}\,\beta_{OH}\,\delta_{ring}$	1033	17		
$\beta_{CH}\,\beta_{OH}$	**1165**	173	1167	1.0
$\beta_{CH}\,\beta_{OH}$	1231	40		
$\beta_{CH}\,\sigma_{CO}$	1255	73		
$\beta_{CH}\,\sigma_{CO}$	**1329**	77	1305	0.1
$\beta_{CH}\,\beta_{OH}\,\sigma_{CC}$	**1391**	36	1367	0.05
$\beta_{CH}\,\beta_{OH}\,\sigma_{CC}$	**1458**	48		
$\beta_{CH}\,\sigma_{CO}\,\sigma_{CC}$	**1493**	103	1450	0.45
$\beta_{CH}\,\sigma_{CC}$	**1519**	100		
$\beta_{CH}\,\beta_{OH}\,\sigma_{CC}$	1540	17		
$\beta_{CH}\,\sigma_{CO}\,\sigma_{CC}$	1626	43		

[a] B3LYP/6-311+G(d,p); frequency values are scaled by a factor of 0.98. [b] β = in plane bend; β' = out of plane bend; σ = stretch; δ = deformation. [c] Bands with I < 15 km/mol are not listed. ν in cm^{-1}; I in km/mol. The vibrational modes that may be assigned to the experimental IRMPD features are highlighted in bold. [d] ν in cm^{-1}; I_{rel} in arbitrary units.

consecutive IRMPD process, as already suggested to account for the behavior of protonated benzaldehyde at higher laser power. However, this possibility appears less likely in the present case. A change in the laser power is of little if any consequence regarding the relative yield of the two fragmentation channels, and more important, the relative abundance of $C_6H_5^+$ fails to show the expected increase in proximity of 1228 and 1433 cm^{-1} that would be expected if $C_6H_7^+$ had the structure of a benzenium ion (Figure 6). In contrast, it may be seen that the relative amount of $C_6H_5^+$ formed is higher in correspondence with the distinct feature at 1167 cm^{-1}. Obviously, the possibility should not be excluded that the $C_6H_7^+$ photofragment from protonated tropone may have a structure different from the $C_6H_7^+$ product of protonated benzaldehyde and therefore the vibrational modes that will be active in forming $C_6H_5^+$ may lie at photon energies different from the ones pertaining to protonated benzene. An answer to this kind of question may possibly be obtained by performing IRMPD of the $C_6H_7^+$ photodissociation product of protonated tropone in an appropriate multistep sequence. Unfortunately the weak

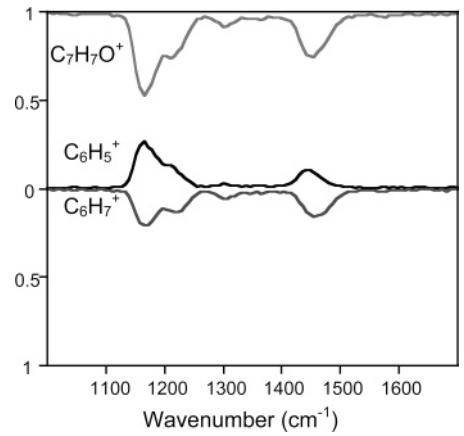

Figure 5. Ion abundances (in arbitrary units) for $[C_7H_7O]^+$ (protonated tropone) and for the fragmentation products ($C_6H_7^+$ and $C_6H_5^+$) plotted as a function of the IR wavenumber.

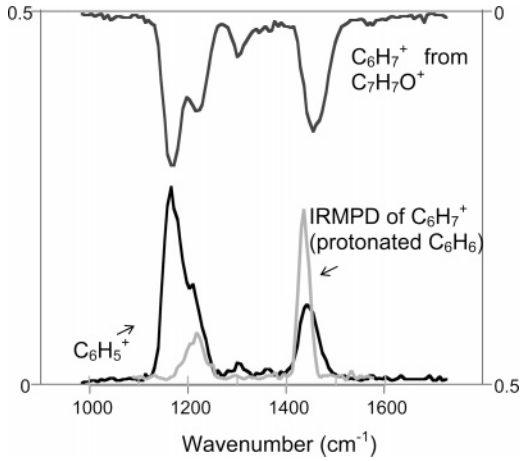

Figure 6. Ion abundances (in arbitrary units) for the formation of $C_6H_7^+$ (ordinate on the right) and $C_6H_5^+$ (ordinate on the left) by IRMPD of protonated tropone, displayed together with the IRMPD spectrum of protonated benzene.[11a]

activity of protonated tropone upon IRMPD prevented the accumulation of $C_6H_7^+$ ions in useful amount to perform further IRMPD. On the basis of the results presently available, the activation of competitive fragmentation pathways appears as

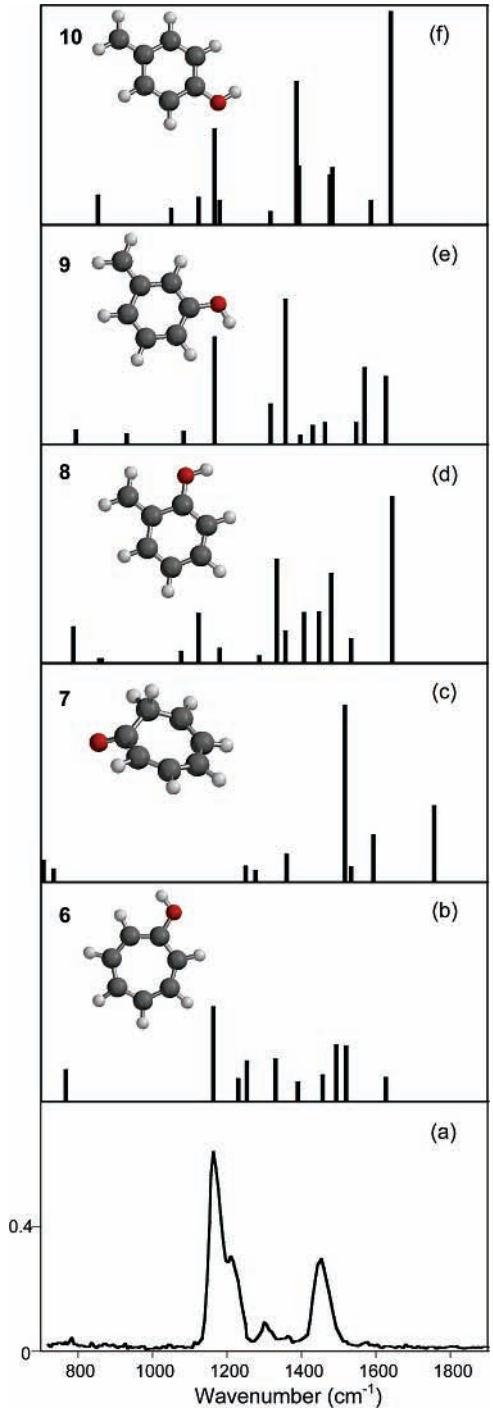

Figure 7. (a) IRMPD spectrum of $[C_7H_7O]^+$ ions from protonated tropone (*R* as a function of IR wavenumber). (b−f) IR stick spectra calculated for **6**−**10**, respectively.

the most likely explanation of the observed IRMPD behavior. The potential energy profile for the dissociation pathways of **6** is not known. However, it is reasonable to expect that the loss of both a CO or a $[H_2CO]$ fragment may involve extensive heavy atom rearrangement associated to significant activation energies. In the assumption that the dissociation products are the same species listed in Table 1, as postulated to arise from protonated benzaldehyde, their relative energies indicate that the $C_6H_5^+$ product channel may be considerably more energy demanding. The red shift displayed by the $C_6H_5^+$ channel is consistent with this reasoning. It has been noted in fact that, in the presence of two competing dissociation processes, the one associated with the highest critical energy may show a larger red shift induced by anharmonicity.[12b] In other words, the $C_6H_5^+$ channel samples $[C_7H_7O]^+$ ions with a higher average internal energy, in a state where anharmonicity effects become evident, shifting the absorption frequency to lower values. As a matter of fact, it has been suggested that differential red shifts along competitive dissociation routes may aid in assessing the anharmonicity parameters when evaluated against the calculated harmonic IR frequency of the specific mode.[12b]

The experimental IRMPD spectrum of $[C_7H_7O]^+$ ions from protonated tropone is displayed in Figure 7a. A comparison with the IRMPD spectrum displayed in Figure 4a clearly indicates that the protonation of tropone yields a species that is easily differentiated by IRMPD from the $[C_7H_7O]^+$ ions obtained by protonation of benzaldehyde. The calculated line spectra of potential isomers **6**−**10** are given in Figure 7b−f. Any significant contribution of a C-protonated isomer such as **7** (Figure 7c) can be discarded since no IRMPD band (Figure 7a) was observed when the IR−FEL laser was in resonance with the characteristic strongly IR-active C═O stretching band of this isomer (1757 cm^{-1}). Similarly, contributions of *ortho*- or *para*-hydroxybenzylium isomers are unlikely since these two isomers are characterized by a strongly IR-active vibrational mode in the region of the infrared spectrum near 1640 cm^{-1} (Figure 7d,f) where no IRMPD band was observed. A significant population of *meta*-hydroxybenzylium isomer **9** should have lead to a strong IRMPD feature at 1357 cm^{-1}, which was not observed experimentally. On the other hand, a fair agreement is provided by the calculated IR spectrum of **6** (Figure 7b) and an assignment of the experimental IRMPD features to the calculated frequencies is presented in Table 3. The two strongest IRMPD features were observed at 1167 and 1450 cm^{-1}. The IRMPD band at 1167 cm^{-1} nicely matches with the position of the most strongly active vibrational mode (1165 cm^{-1}) of the hydroxytropylium isomer 6 (Figure 7b). The feature observed at 1450 cm^{-1}, on the other hand, could be the result of an IR absorption process through three closely spaced active modes (Table 3), including two presenting a calculated IR activity greater that 100 km/mol. Additional evidence on the tropylium ion structure may be gained in future work extending the spectroscopic study to the CH and OH stretching region of the IR spectrum, where aromatic CH and allylic CH vibrations should be easily discriminated.

As a final note, the IRMPD efficiency was much greater for $[C_7H_7O]^+$ ions resulting from the protonation of benzaldehyde than from the protonation of tropone. As a result, weakly active IR vibrational modes such as the one at 767 cm^{-1} of isomer 6 associated with a calculated IR intensity of 56 km/mol (Table 3) could not be revealed, while a vibrational mode (774 cm^{-1}, Table 2) of isomer **1**-*cis* associated with the same intensity (56 km/mol) led to a significant IRMPD signal in the case of protonated benzaldehyde.

Conclusions

The present IRMPD investigation of gaseous protonated benzaldehyde presents an interesting case of a simple mono-substituted benzene species, undergoing exclusively protonation at the formyl substituent under the operating conditions adopted. Previous IRMPD studies exploiting the CLIO IR−FEL radiation were successful in characterizing protonated aromatic molecules ranging from the prototypical benzenium ion,[11a] to *ortho*/*para* protonated species from fluorobenzene or toluene,[11b,d] and to *ipso* protonated species in the presence of a SiH_3 group as phenyl ring substituent.[11c] A carbonyl protonated structure was tentatively assigned to protonated benzoic acid when its IRMPD

spectrum was evaluated against the calculated spectra of a few different possible structures. However, so far potentially diagnostic methods for assigning structures to gaseous ions have failed to provide a clear-cut answer when confronted with the $[C_7H_7O]^+$ ions generated from a variety of different precursors. The present IRMPD spectroscopic investigation has allowed us to obtain unambiguous evidence that $[C_7H_7O]^+$ ions from protonated benzaldehyde show the features of the **1**-*cis* protonated isomer with a possible but only minor contribution of **1**-*trans*. This result is remarkable in consideration of the small energy difference between the two species which are separated, however, by a substantial barrier for the interconversion by C−O bond rotation. The same IRMPD assay has been exploited for characterizing $[C_7H_7O]^+$ ions from the protonation of tropone. The so-formed ions display features that are best accounted for by an O-protonated species, **6**, thus proving the value of IRMPD as a tool for structure characterization and assignment. The two O-protonated isomers appear to be stable with respect to conceivable skeletal isomerization processes that could be allowed by the exothermicity of their formation process. As a final note, **1**-*cis* and **6** are hydroxy-substituted benzylium and tropylium ions, respectively, and close relatives to a class of ions ($C_7H_7^+$) that are perhaps the most studied species in gas-phase ion chemistry and mass spectrometry in general.[25] Recently, the gas-phase IR spectra of neutral C_7H_7• isomers have been measured using an IR−UV double resonance scheme.[26] However, preliminary efforts toward probing the IR spectral features of $C_7H_7^+$ isomers by IRMPD have met with only partial success.[27] Thus, the present characterization of hydroxy-substituted tropylium and benzylium ions provides the first IRMPD data in the so-called IR fingerprint range regarding members of this important family of ionic intermediates.

Acknowledgment. This work was supported by the CNRS, the laser center POLA at the Université Paris Sud 11, the Italian MIUR, and the Deutsche Forschungsgemeinschaft (Grants DO 729/2-2 and DO 729/1-2). We thank Jean-Michel Ortega, François Glotin, and the CLIO team for their support during the experiments. We are grateful to Gérard Mauclaire, Michel Heninger, Gerard Bellec, and Pierre Boissel, who, together with J.L., provided us with the mobile FT-ICR mass spectrometer used in this work. Financial support by the European Commission is also gratefully acknowledged.

References and Notes

(1) (a) Brouwer, D. M.; Mackor, E. L.; MacLean, C. Arenonium Ions. In *Carbonium Ions*; Olah, G. A., Schleyer, P. v. R., Eds.; Wiley: New York, 1970; Vol II. (b) Smith, M. B.; March, J. *Advanced Organic Chemistry. Reactions, Mechanisms, and Structure*, 5th ed.; Wiley: New York, 2001; Chapter 11. (c) Taylor, R. *Electrophilic Aromatic Substitution*; John Wiley & Sons Ltd.: Chichester, U.K., 1990.

(2) (a) Cacace, F. *Acc. Chem. Res.* **1988**, *21*, 215. (b) Kuck, D. *Mass Spectrom. Rev.* **1990**, *9*, 583. (c) Fornarini, S. *Mass Spectrom. Rev.* **1996**, *15*, 365. (d) Fornarini, S.; Crestoni, M. E. *Acc. Chem. Res.* **1998**, *31*, 827. (e) Kuck, D. Protonated Aromatics and Arenium Ions. In *The Encyclopedia of Mass Spectrometry, Fundamentals and Applications to Organic (and Organometallic) Compounds*; Elsevier: Oxford, U.K., 2005; Vol. 4, p 229.

(3) (a) Cassady, C. J.; Freiser, B. S.; Russell, D. H. *Org. Mass Spectrom.* **1983**, *18*, 378. (b) Russel, D. H.; Freiser, B. S.; McBay, E. H.; Canada, D. C. *Org. Mass Spectrom.* **1983**, *18*, 474.

(4) (a) Freiser, B. S.; Woodin, R. L.; Beauchamp, J. L. *J. Am. Chem. Soc.* **1975**, *97*, 6893. (b) Kuck, D.; Ingemann, S.; De Koning, L.; Grützmacher, H.-F.; Nibbering, N. M. M. *Angew. Chem., Int. Ed. Engl.* **1985**, *24*, 693. (c) Ni, J.; Harrison, A. G. *Can. J. Chem.* **1995**, *73*, 1779.

(5) Chiavarino, B.; Crestoni, M. E.; Di Rienzo, B.; Fornarini, S. *J. Am. Chem. Soc.* **1998**, *120*, 10856.

(6) (a) Dunbar, R. C. *Int. J. Mass Spectrom.* **2000**, *200*, 571. (b) Duncan, M. A. *Int. J. Mass Spectrom.* **2000**, *200*, 545. (c) Bieske, E. J.; Dopfer, O. *Chem. Rev.* **2000**, *100*, 3963. (d) Dopfer, O. *Z. Phys. Chem.* **2005**, *219*, 125. (e) Duncan, M. A. *Int. Rev. Phys. Chem.* **2003**, *22*, 407. (f) Oomens, J.; Tielens, A. G. G. M.; Sartakov, B.; von Helden, G.; Meijer, G. *Astrophys. J.* **2003**, *591*, 968.

(7) (a) Okumura, M.; Yeh, L. I.; Myers, J. D.; Lee, Y. T. *J. Chem. Phys.* **1986**, *85*, 2328. (b) Yeh, L. I.; Okumura, M.; Myers, J. D.; Price, J. M.; Lee, Y. T. *J. Chem. Phys.* **1989**, *91*, 7319.

(8) (a) Dopfer, O.; Olkhov, R. V.; Maier, J. P. *J. Chem. Phys.* **1999**, *111*, 10754. (b) Bakker, J. M.; Satink, R. G.; von Helden, G.; Meijer, G. *Phys. Chem. Chem. Phys.* **2002**, *4*, 24. (c) Satink, R. G.; Meijer, G.; von Helden, G. *Chem. Phys. Lett.* **2003**, *371*, 469. (d) Fujimaki, E.; Fujii, A.; Ebata, T.; Mikami, N. *J. Phys. Chem. A* **2001**, *105*, 4882. (e) Fujii, A.; Fujimaki, E.; Ebata, T.; Mikami, N. *J. Chem. Phys.* **2000**, *112*, 6275. (f) Horia-Sorin, A.; Solcà, N.; Dopfer, O. *J. Phys. Chem. A* **2005**, *109*, 3598. (g) Solcà, N.; Dopfer, O. *J. Chem. Phys.* **2004**, *120*, 10470. (h) Satink, R. G.; Piest, H.; von Helden, G.; Meijer, G. *J. Chem. Phys.* **1999**, *111*, 10750.

(9) (a) Solcà, N.; Dopfer, O. *J. Am. Chem. Soc.* **2004**, *126*, 1716. (b) Solcà, N.; Dopfer, O. *Chem.—Eur. J.* **2003**, *9*, 3154. (c) Solcà, N.; Dopfer, O. *Angew. Chem., Int. Ed.* **2003**, *42*, 1537. (d) Solcà, N.; Dopfer, O. *Angew. Chem., Int. Ed.* **2002**, *41*, 3628. (d) Solcà, N.; Dopfer, O. *Chem. Phys. Lett.* **2001**, *342*, 191. (e) Solcà, N.; Dopfer, O. *Chem. Phys. Chem.* **2005**, *6*, 434.

(10) (a) Oomens, J.; Sartakov, B. G.; Tielens, A. G. G. M.; Meijer, G.; von Helden, G. *Astrophys. J.* **2001**, *560*, L99. (b) Oomens, J.; Meijer, G.; von Helden, G. *J. Phys. Chem. A* **2001**, *105*, 8302. (c) Oomens, J.; Van Roij, A. J. A.; Meijer, G.; Von Helden, G. *Astrophys. J.* **2000**, *542*, 404.

(11) (a) Jones, W.; Boissel, P.; Chiavarino, B.; Crestoni, M. E.; Fornarini, S.; Lemaire, J.; Maitre, P. *Angew. Chem., Int. Ed.* **2003**, *42*, 2057. (b) Solcà, N.; Dopfer, O.; Lemaire, J.; Maître, P.; Crestoni, M. E.; Fornarini, S. *J. Phys. Chem. A* **2005**, *109*, 7881. (c) Chiavarino, B.; Crestoni, M. E.; Fornarini, S.; Lemaire, J.; MacAleese, L.; Maitre, P. *ChemPhysChem* **2005**, *6*, 437. (d) Dopfer, O.; Lemaire, J.; Maître, P.; Chiavarino, B.; Crestoni, M. E.; Fornarini, S. *Int. J. Mass Spectrom.* **2006**, *249*−*250*, 149. (e) Dopfer, O. *J. Phys. Org. Chem.* **2006**, in press.

(12) (a) Oomens, J.; von Helden, G.; Meijer, G. *J. Phys. Chem. A* **2004**, *108*, 8273. (b) Oomens, J.; Moore, D. T.; Meijer, G.; von Helden, G. *Phys. Chem. Chem. Phys.* **2004**, *6*, 710. (c) Oomens, J.; Bakker, J. M.; Sartakov, B. G.; Meijer, G.; von Helden, G. *Chem. Phys. Lett.* **2003**, *367*, 576.

(13) Mauclaire, G.; Lemaire, J.; Boissel, P.; Bellec, G.; Heninger, M. *Eur. J. Mass Spectrom.* **2004**, *10*, 155.

(14) (a) Maître, P.; Le Caër, S.; Simon, A.; Jones, W.; Lemaire, J.; Mestdagh, H.; Heninger, M.; Mauclaire, G.; Boissel, P.; Prazeres, R.; Glotin, F.; Ortega, J.-M. *Nucl. Instrum. Methods Phys. Res. A* **2003**, *507*, 541. (b) Lemaire, J.; Boissel, P.; Heninger, M.; Mauclaire, G.; Bellec, G.; Mestdagh, H.; Simon, A.; Le Caër, S.; Ortega, J.-M.; Glotin, F.; Maître, P. *Phys. Rev. Lett.* **2002**, *89*, 273002.

(15) (a) Reed, C. A.; Fackler, N. L. P.; Kim, K.-C.; Stasko, D.; Evans, D. R.; Boyd, P. D. W.; Rickard, C. E. F. *J. Am. Chem. Soc.* **1999**, *121*, 6314. (b) Reed, C. A.; Kim, K.-C.; Stoyanov, E. S.; Stasko, D.; Tham, F. S.; Mueller, L. J.; Boyd, P. D. W. *J. Am. Chem. Soc.* **2003**, *125*, 1796. (c) Kato, T.; Stoyanov, E.; Geier, J.; Grützmacher, H.; Reed, C. A. *J. Am. Chem. Soc.* **2004**, *126*, 12451. (d) Stasko, D.; Reed, C. A. *J. Am. Chem. Soc.* **2002**, *124*, 1148. (e) Davlieva, M. G.; Lindeman, S. V.; Neretin, I. S.; Kochi, J. K. *J. Org. Chem.* **2005**, *70*, 4013.

(16) (a) Prazeres, R.; Glotin, F.; Insa, C.; Jaroszynski, D. A.; Ortega, J. M. *Eur. Phys. J. D* **1998**, *3*, 87. (b) Glotin, F.; Ortega, J. M.; Prazeres, R.; Rippon, C. *Nucl. Instrum. Methods B* **1998**, *144*, 8.

(17) (a) Scott, A. P.; Radom, L. *J. Phys. Chem.* **1996**, *100*, 16502. (b) Andersson, M. P.; Uvdal, P. *J. Phys. Chem. A* **2005**, *109*, 2937. (c) Halls, M. D.; Velkovski, J.; Schlegel, H. B. *Theor. Chem. Acc.* **2001**, *105*, 413. (d) Langhoff, S. R. *J. Phys. Chem.* **1996**, *100*, 2819.

(18) Hunter, E. P.; Lias, S. G. *Proton Affinity Evaluation In NIST Chemistry WebBook*; Linstrom, P. J., Mallard, W. G., Eds.; NIST Standard Reference Database Number 69; National Institute of Standards and Technology: Gaithersburg, MD (http://webbook.nist.gov), Jun 2005.

(19) (a) Lee, I.; Kim, C. K. *J. Phys. Chem. A* **2000**, *104*, 6332. (b) Levy, J. B. *Struct. Chem.* **2000**, *11*, 141. (c) Kovacevic, B.; Liebman, J.; Maksić, Z. B. *J. Chem. Soc., Perkin Trans. 2* **2002**, 1544.; (d) Maksiæ, Z. B.; Eckert-Maksić, M. *Theoretical Organic Chemistry, Theoretical and Computational Chemistry*; Pàrkànyi, C., Ed.; Elsevier: New York, 1998; Vol. 5. (e) Antol, I.; Eckert-Maksić, M.; Klessinger, M. *J. Mol. Struct. (THEOCHEM)* **2003**, *664*−*665*, 309.

(20) Olah, G. A.; Rasul, G.; York, C.; Prakash, G. K. S. *J. Am. Chem. Soc.* **1995**, *117*, 11211.

(21) Miller, S. R.; Krasutsky, S.; Kiprof, P. *J. Mol. Struct. (THEOCHEM)* **2004**, *674*, 43.

(22) (a) Filges, U.; Grützmacher, H.-F. *Org. Mass Spectrom.* **1986**, *21*, 673. (b) Shannon, J. S. *Aust. J. Chem.* **1962**, *15*, 265.

(23) (a) Fridgen, T. D.; MacAleese, L.; McMahon, T. B.; Lemaire, J.; Maître, P. *Phys. Chem. Chem. Phys.* **2006**, *8*, 955.; (b) Simon, A.; Ortega, J.-M.; Boissel, P.; Lemaire, J.; Maître, P. *J. Am. Chem. Soc.* **2004**, *126*, 11666. (c) Reinhard, B. M.; Lagutschenkov, A.; Lemaire, J.; Boissel, P.; Maitre, P.; Niedner-Schatteburg, G. *J. Phys. Chem. A* **2004**, *108*, 3350. (d) Dunbar, R. C.; Moore, D. T. Oomens, J. *J. Phys. Chem. A* **2006**, *110*, published on the Web Mar 2006.

(24) This effect has also been seen already in single photon IRPD of ligand tagged clusters where hot clusters evaporate more ligands than cold clusters and spectra recorded in different fragment channels may look very different: (a) Nizkorodov, S. A.; Dopfer, O.; Ruchti, T.; Meuwly, M.; Maier, J. P.; Bieske, E. J. *J. Phys. Chem.* **1995**, *99*, 17118. (b) Dopfer, O.; Olkhov, R. V.; Maier, J. P. *J. Chem. Phys.* **1999**, *111*, 10754.

(25) (a) Kuck, D. *Mass Spectrom. Rev.* **1990**, *9*, 187. (b) Kuck, D. Tropylium and Related Ions. In *Encyclopedia* of *Mass Spectrometry*; Nibbering, N. M. M., Ed.; Elsevier: Amsterdam, 2005; Vol. 4. (c) Lifshitz, C. *Acc. Chem. Res.* **1994**, *27*, 138. (d) Moon, J. H.; Choe, J. C.; Kim, M. S. *J. Phys. Chem. A* **2000**, *104*, 458. (e) Fati, D.; Lorquet, A. J.; Locht, R.; Lorquet, J. C.; Leyh, B. *J. Phys. Chem. A* **2004**, *108*, 9777. (f) Fridgen, T. D.; Troe, J.; Viggiano, A. A.; Midey, A. J.; Williams, S.; McMahon, T. B. *J. Phys. Chem. A* **2004**, *108*, 5600.

(26) Satink, R. G.; Meijer, G.; von Helden, G. *J. Am. Chem. Soc.* **2003**, *125*, 15714.

(27) Some of the authors of this paper (O.D., J.L., P.M.) have recorded the IRMPD spectrum of tropylium (c-$C_7H_7^+$) already in May 2004.